Cell, Vol. 107, 751–762, December 14, 2001, Copyright ©2001 by Cell Press

Functional Link between the Mammalian Exosome and mRNA Decapping

Zuoren Wang and Megerditch Kiledjian[1]
Department of Cell Biology and Neuroscience
Rutgers University
604 Allison Road
Piscataway, New Jersey 08854

Summary

Mechanistic understanding of mammalian mRNA turnover remains incomplete. We demonstrate that the 3′ to 5′ exoribonuclease decay pathway is a major contributor to mRNA decay both in cells and in cell extract. An exoribonuclease-dependent scavenger decapping activity was identified that follows decay of the mRNA and hydrolyzes the residual cap. The decapping activity is associated with a subset of the exosome proteins in vivo, implying a higher-order degradation complex consisting of exoribonucleases and a decapping activity, which together coordinate the decay of an mRNA. These findings indicate that following deadenylation of mammal mRNA, degradation proceeds by a coupled 3′ to 5′ exoribonucleolytic activity and subsequent hydrolysis of the cap structure by a scavenger decapping activity.

Introduction

All eukaryotic mRNAs are modified at the 5′ end with the addition of a cap structure. In nearly all cases the cap consists of a guanine nucleoside methylated at the N-7 position (m^7G) covalently attached to the terminal nucleoside of the RNA with an unusual 5′-5′ linkage (Shatkin, 1976). The 3′ ends of most mRNA are also modified and contain a stretch of adenosine residues (Sachs, 1993). Both of these structures serve to protect the respective ends of the mRNA from exoribonucleolytic degradation (Ross, 1995), are involved in transport of the mRNA to the cytoplasm (Izaurralde et al., 1995; Jarmolowski et al., 1994; Wickens and Gurdon, 1983), and contribute to translation of the mRNA (Gingras et al., 1999; Hentze, 1997; Sachs et al., 1997). A role for the cap has also been demonstrated in the splicing of pre-mRNA (Konarska et al., 1984). The 5′ cap is bound by a cap binding heterodimeric complex consisting of CBC20 and CBC80 in the nucleus (Izaurralde et al., 1994) and by the cytoplasmic cap binding protein eIF4E in the cytoplasm (Gingras et al., 1999).

The protein components and the mechanism of m^7G cap addition have been extensively characterized in many species (Furuichi and Shatkin, 2000). In contrast, much less is known about the mechanism involving removal of the cap. Much of our understanding of decapping comes from work in the yeast *Saccharomyces cerevisiae* where the gene encoding the decapping enzyme Dcp1p has been cloned (Beelman et al., 1996). Dcp1p is a pyrophosphatase that decaps the mRNA by releasing m^7GDP. This activity preferentially hydrolyzes methylated cap and requires an RNA longer than 25 nucleotides (LaGrandeur and Parker, 1998). Auxiliary factors that augment the function of Dcp1p have also been identified (Bonnerot et al., 2000; Bouveret et al., 2000; Dunckley and Parker, 1999; Zhang et al., 1999a). Recently, a putative mammalian activity functionally equivalent to the yeast Dcp1p was identified (Gao et al., 2001). A mammalian decapping activity that functions on capped oligonucleotides that are shorter than 10 nucleotides in length has also been reported and proposed to clear exoribonucleolytic products that retain a cap structure (Nuss et al., 1975).

The pathway of mRNA turnover is also best studied in yeast and predominantly involves removal of the poly(A) tail followed by decapping (Decker and Parker, 1993; Muhlrad et al., 1994). The poly(A) tail is initially deadenylated to an oligo(A), which renders the mRNA susceptible to decapping by Dcp1p (Beelman et al., 1996). The exposed 5′ end is subsequently degraded by Xrn1, a 5′ to 3′ exoribonuclease (Hsu and Stevens, 1993). An alternative pathway also exists where a complex of proteins (termed the exosome) degrade the mRNA in a 3′ to 5′ direction following deadenylation (Anderson and Parker, 1998; Mitchell et al., 1997). The exosome also plays a significant role in a nuclear discard pathway to clear unspliced pre-mRNA in yeast (Bousquet-Antonelli et al., 2000).

We have developed an in vitro mRNA decay assay that recapitulates regulated mRNA turnover including PABP-dependent deadenylation (Wang et al., 1999; Wang and Kiledjian, 2000b). Using this system, we now present evidence that mammalian mRNA turnover can proceed through a coupled 3′ to 5′ exonuclease degradation-dependent decapping pathway.

Results

Capped and Polyadenylated RNA Is More Stable than Uncapped and Polyadenylated RNA In Vitro

We recently reported an in vitro mRNA decay system that recapitulated regulated mRNA turnover by using the α globin transcript as a model system. Consistent with previous demonstrations of mRNA turnover in cells, the initial step for the degradation of RNA in this system is the removal of the poly(A) tail (Wang et al., 1999). We now address more general mechanistic questions of mRNA turnover in mammals. We first asked whether the in vitro system recapitulates the differential stability observed in cells between capped and uncapped mRNA (Drummond et al., 1985; Furuichi et al., 1977; Green et al., 1983; Krieg and Melton, 1984). We used the pcDNA3 polylinker (pcP) region as a generic RNA substrate and carried out the reactions in human erythroleukemia K562 cytosolic S130 extract. The RNA was transcribed, with or without cap analog, in the presence of [α-^{32}P]UTP from a template that introduced 60 adenosine residues at the 3′ end. As shown in Figure 1A, capped RNA was more stable, with a half-life greater than the 2 hr reaction

[1] Correspondence: kiledjia@biology.rutgers.edu

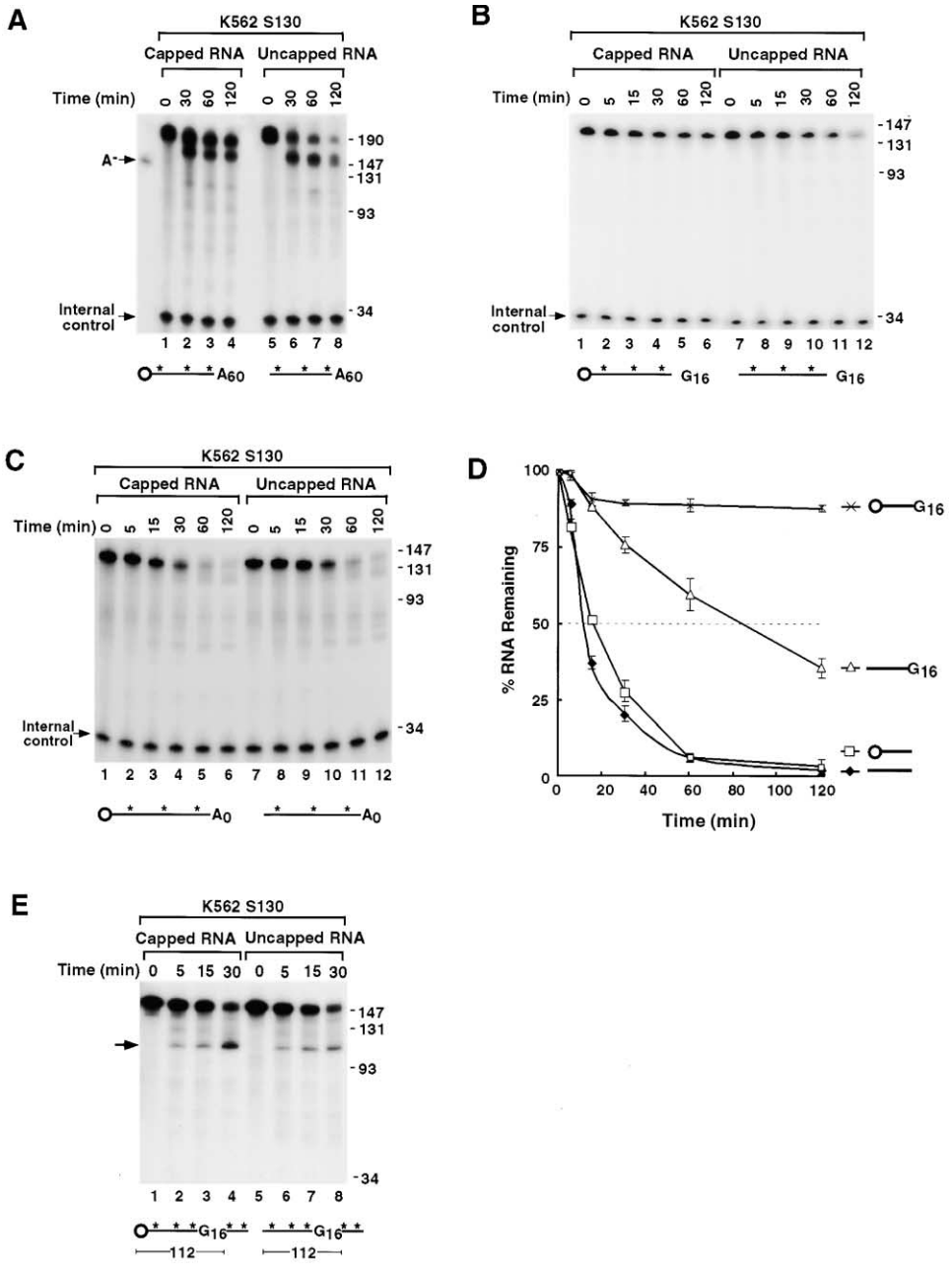

Figure 1. 3′ to 5′ RNA Degradation Is More Prominent than 5′ to 3′ Degradation In Vitro

(A) Uniformly labeled capped and uncapped polyadenylated pcP RNA were used in an in vitro decay assay with K562 S130 extract for the indicated times, and the RNA products were resolved on a denaturing 7 M urea/8% polyacrylamide gel and visualized by autoradiography. Migration of the unadenylated pcP RNA (A^-) and migration of an internal control oligonucleotide, which was included in the stop buffer to enable quantitation, are indicated on the left. The DNA size markers are shown on the right in nucleotides. The RNA substrate is schematically denoted beneath each panel, and the asterisks represent the position of the ^{32}P labeling. The RNA cap is represented by a circle. The line depicts the RNA, and the extent of polyadenylation is denoted by the "A" with the number of nucleotides shown as a subscript.

(B) In vitro decay reactions with capped or uncapped pcP RNAs containing a G_{16} track on the 3′ end were carried out in K562 S130 extract.

(C) In vitro decay reactions with capped or uncapped unadenylated pcP RNAs were carried out in K562 S130 extract.

(D) The data presented in (B) and (C) are plotted from three independent experiments with the corresponding error bars. The RNAs are depicted schematically on the right. Quantitation from (A) using polyadenylated RNA were not included in the graph since they are similar to results obtained for RNA containing a G_{16} track (B).

(E) Capped and uncapped pcP RNA containing an internal G_{16} track at position 96 were used in an in vitro decay reaction with K562 S130 extract. The RNA and the band corresponding to the blocked intermediate from the 3′ end is schematically depicted on the bottom (112 nucleotides) and denoted by an arrow on the left.

time, while the half-life of the uncapped RNA was approximately 60 min. The differential stability of the two RNAs that differ only by the presence or absence of the 5′ cap suggests that a 5′ to 3′ exoribonuclease activity contributes to the turnover observed in these reactions. Furthermore, both RNAs degraded through a deadenylation process, as indicated by the presence of the phased poly(A) plus intermediate which we have previously shown is due to sequential removal of PABP and rapid decay of the RNA upon removal of the terminal PABP (Wang et al., 1999).

The presence of a 5′ to 3′ exoribonuclease activity was tested by placing a G track on the 3′ end of the RNA to inhibit 3′ to 5′ exoribonuclease activity. Poly(G) stretches have been shown to efficiently block exoribonucleases in yeast (Muhlrad et al., 1994). Capped and uncapped pcP RNAs containing 16 guanosine nucleotides (G_{16}) at their 3′ end were generated (pcP-G_{16}). As can be seen in Figure 1B and presented in graph form in Figure 1D, both RNAs are relatively stable when the 3′ end is protected. However, the differential stability between the capped and uncapped RNAs, which was observed with the polyadenylated RNAs, is maintained. Similar results were also obtained by placing a stable stem loop structure at the 3′ end or by using polyadenylated RNAs in an extract depleted for the deadenylating nuclease PARN (data not shown). The half-life of the capped RNA with a G_{16} track is greater than the 2 hr time course of the experiment, while the half-life of the uncapped RNA with a G_{16} is 90 min (Figure 1D). These results are consistent with the presence of 5′ to 3′ exoribonucleases in mammalian cells.

3′ to 5′ Exoribonuclease Activity Is a Major Contributor to RNA Decay in Mammalian Extract

The relative contribution of the different exoribonuclease activities to RNA degradation was next addressed. The relative stability of capped and uncapped RNAs lacking a poly(A) tail is presented in Figure 1C. Both RNAs were equally unstable, with half-lives of less than 20 min. Similar results were also observed with longer RNAs (data not shown). Quantitations of the results presented in Figures 1B and 1C using capped or uncapped RNAs containing or lacking a G_{16} track block at the 3′ end are plotted in Figure 1D. Quantitations for the polyadenylated RNAs (Figure 1A) were indistinguishable from the G_{16}-containing RNA and were omitted from the graph. A comparison of the half-life for the 5′ end protected capped pcP RNA to that of the 3′ end protected uncapped pcP-G_{16} RNA, indicated a 5-fold greater contribution to the degradation of the RNA from the 3′ end. These results suggest that the 3′ to 5′ exoribonuclease activity is the major contributor to RNA degradation in mammalian extract.

To further substantiate the directionality of the degradation in extract, the G_{16} track was inserted internally within the RNA at nucleotide 96. A block of 5′ to 3′ degradation would generate a 56 nucleotide intermediate, while a block of decay from the 3′ end would generate a 112 nucleotide intermediate. As shown in Figure 1E, the 112 nucleotide band accumulates over time when capped RNA is used, corresponding to a block of 3′ to 5′ exoribonucleases (lanes 2–4). A similar result was also observed with uncapped RNA (lanes 6–8), further supporting the significant role of 3′ to 5′ exoribonucleases. Upon overexposure of the gel, a minor band in the 56 nucleotide range corresponding to a 5′ end block can be detected with the uncapped RNA consistent with the minor contribution for this activity.

3′ to 5′ Exoribonucleases Are Major Contributors to mRNA Decay in Mammalian Cells

To determine whether 3′ to 5′ exoribonucleases are major contributors in intact cells, we introduced a similar set of [^{32}P]RNAs into K562 cells and followed their fate over time. A set of six RNAs were electroporated into cells as described in Experimental Procedures. The RNAs either contained or lacked an m^7G cap at the 5′ end and either lacked or contained a poly(A) tail or a G_{16} track at the 3′ end. Cells were harvested at various times up to 6 hr postelectroporation, and the RNA were resolved and visualized. Similar to the results observed in the in vitro decay system, RNAs containing a block on the 3′ end were more stable than RNAs containing a block on the 5′ end (Figure 2). The half-life of the RNA protected at the 5′ end with a cap but lacking a block on the 3′ end is approximately 60 min (Figures 2A and 2D). The half-life of an RNA lacking a cap and protected with a G_{16} track on the 3′ end is over 3-fold higher (Figures 2B and 2D), while a polyadenylated RNA is more than 4-fold more stable (Figure 2C). These data support the conclusion that degradation from the 3′ end of an mRNA is a major decay pathway in cells as well. Also similar to the in vitro results, polyadenylated RNAs appear to undergo deadenylation as the first step in the decay process, and the deadenylation was indistinguishable regardless of the presence or absence of the 5′ cap.

The above experiments were carried out with RNA introduced into cells. We were also interested in determining whether an endogenous mRNA undergoes a predominant 3′ to 5′ decay. To assess the decay pathway of an endogenous mRNA, we arbitrarily chose c-*myc*, a relatively short-lived mRNA, to enable detection of decay products within a manageable experimental time frame. RNA was isolated from K562 cells at various times following Actinomycin D treatment and was analyzed by RNase protection assays (RPA) using two different probes. One probe was complementary to the 5′ end of the mRNA, and the second was complementary to the 3′ end. We reasoned that RPA might be sensitive enough to detect the rare intermediates that are in the process of being degraded from one end or the other despite the rapid action of exoribonucleases. If the RNAs were degraded predominantly from the 3′ end, the relative ratio of mRNAs containing the 3′ end would be less than that containing the 5′ end. The opposite would be true if the decay occurred from the 5′ end. Cytoplasmic RNA was used in the analysis to eliminate potential complications of trapped transcription intermediates upon transcription arrest. As shown in Figure 2E (lanes 6–10 and graph), the relative ratio of mRNAs containing an intact 3′ end relative to an intact 5′ end decreased over time, indicating that the mRNA is predominantly degraded from the 3′ end. Similar results were also detected using HeLa cells (Figure 2E, lanes 11–15). These results are consistent with the directionality of c-*myc*

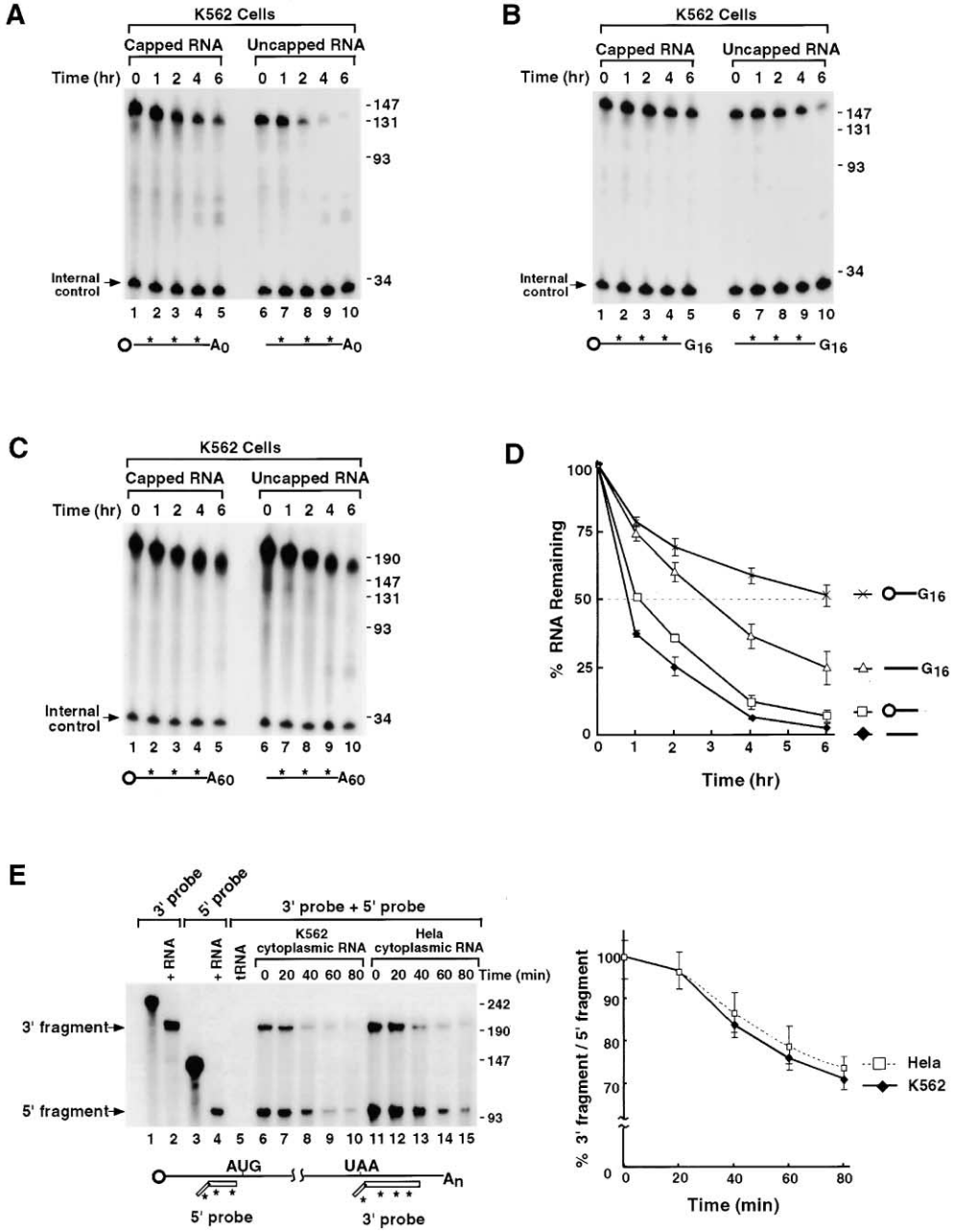

Figure 2. 3′ to 5′ Degradation of RNAs in Cells

Capped and uncapped ^{32}P uniformly labeled pcP RNAs containing or lacking a block on the 3′ end were introduced into cells, and the half-lives were determined. Uniformly labeled capped and uncapped pcP RNAs were transfected into K562 cells, and the RNA products were isolated at the indicated times and resolved as described in the legend to Figure 1.

(A) RNAs lacking a structure on the 3′ end.

(B) RNAs containing a G_{16} track on the 3′ end.

(C) RNAs containing a poly(A) tail at the 3′ end.

(D) The data presented in (A) and (B) are plotted. The numbers were derived from three independent experiments, and error bars are shown.

(E) RPA to detect the presence of the 5′ end (nucleotides 249–350) and the 3′ end (nucleotides 1829–2032) of the c-*myc* mRNA were carried out with cytoplasmic RNA from K562 cells (lanes 6–10) or HeLa cells (lanes 11–15) following the indicated times of Actinomycin D treatment. The bands corresponding to the 5′ fragment or the 3′ fragment are indicated on the left, and the location of the probes relative to the translation start site (AUG) and stop codon (UAA) are shown schematically on the bottom. Quantitations from three independent experiments were plotted as a percent of the 3′ fragment to the 5′ fragment. The ratio at time zero was set to 100%.

mRNA decay reported in vitro (Brewer, 1998). Collectively, our data demonstrates that, with both RNA introduced into cells and endogenous mRNA, the primary direction of decay is from the 3′ end of the mRNA.

The Presence of a Degradation-Dependent Decapping Activity in Human Cells

RNA decapping activity has been demonstrated in the yeast *Saccharomyces cerevisiae*. Dcp1p can hydrolyze

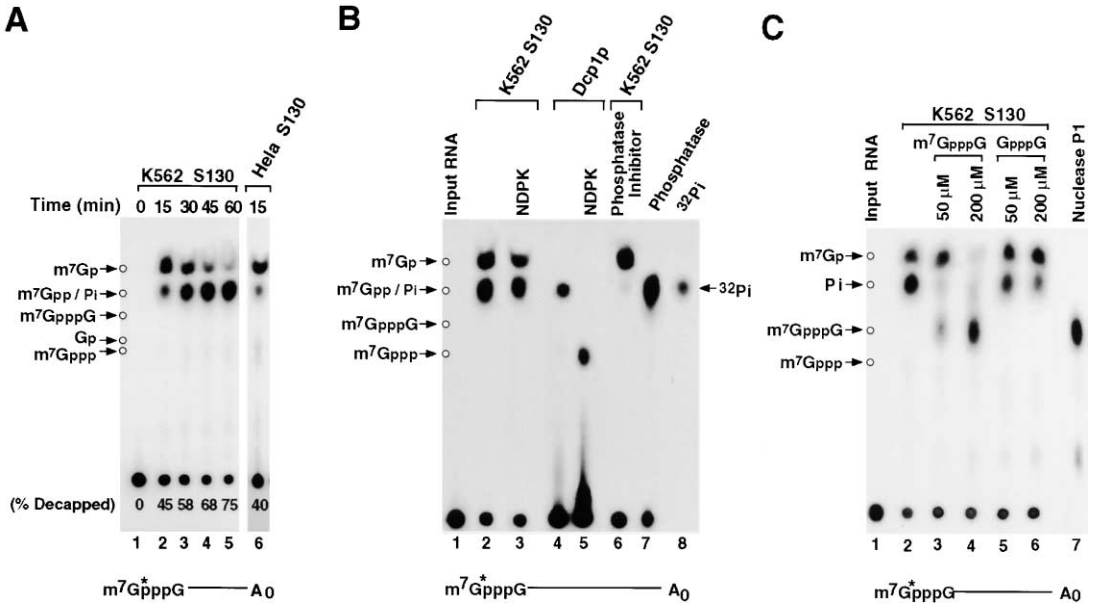

Figure 3. Detection of a Methyl Cap-Specific Decapping Activity in Mammalian S130 Extract

Unadenylated and cap-labeled pcP RNA was used in decay assays to detect decapping activity in S130 extract.

(A) In vitro decay assays were carried out by incubating cap-labeled (m^7G^*pppG-) pcP RNA with K562 (lanes 2–5) or HeLa (lane 6) S130 extract at 37°C for the indicated times. Reaction products were resolved on PEI TLC plates. Standards were developed on the TLC simultaneously and visualized by ultraviolet shadowing, and their migration is indicated on the left. The percent of input RNA that was decapped (where the sum of both decapping products was used) is indicated. The RNA used in the reaction is schematically depicted on the bottom where the cap is represented by the m^7GpppG and the asterisk denotes the labeled phosphate.

(B) An in vitro decay assay was carried out with 5′ cap-labeled pcP RNA in K562 S130 extract. The products from lane 2 were treated with either nucleoside diphosphate kinase (NDPK; lane 3) or calf intestinal phosphatase (lane 7). A decay reaction carried out with extract containing a phosphatase inhibitor cocktail is shown in lane 6. The Dcp1p decapping product is shown in lane 4, and its treatment with NDPK is presented in lane 5. Inorganic phosphate (^{32}Pi) is shown in lane 8. Migration of the cold standards are indicated on the left, and a schematic of the pcP RNA is shown on the bottom.

(C) In vitro decay assays using unadenylated, cap-labeled pcP RNA (shown on the bottom) were carried out for 30 min at 37°C in K562 S130 extract (lane 2) with the indicated amount of m^7GpppG cap analog (lanes 3 and 4) or unmethylated GpppG cap analog (lanes 5 and 6). Resolution of nuclease P1-treated substrate RNA is shown in lane 7. Nuclease P1 degrades the phosphodiester bonds within the body of the RNA to release the cap (m^7GpppG).

the m^7G cap structure on the 5′ end of an mRNA to release m^7GDP (Beelman et al., 1996). A decapping activity has also been reported in mammalian cells, but this activity releases m^7GMP (Nuss et al., 1975). We were interested in determining whether a decapping activity was present in the in vitro decay system and how such an activity would coincide with the above observation that 3′ to 5′ degradation was the prominent decay activity. The pcP RNA, which is 136 nucleotides long, was used as a substrate. The RNA was capped with [α-^{32}P]GTP using the vaccinia capping enzyme, which labels the cap at the first phosphate following the methylated guanosine (m^7G^*pppG; see Experimental Procedures). The RNA was used in an in vitro decay assay as above.

A time course in vitro decay reaction was carried out with cap-labeled unadenylated pcP RNA for up to one hour in cytoplasmic K562 S130 extract. The potential pyrophosphatase decapping products were resolved by polyethyleneimine (PEI)-cellulose thin-layer chromatography (TLC) (Beelman et al., 1996; Zhang et al., 1999b). Two spots were detected (Figure 3A; lanes 2–5). The top spot comigrated with the m^7GMP standard, while the second spot comigrated with the m^7GDP standard as well as inorganic phosphate (see below). The m^7GMP was the predominant product at the earlier time, while the lower spot accumulated with longer incubation times. By 1 hr, 75% of the input RNA was decapped. A similar activity was also detected in HeLa cells (lane 6). These data demonstrate that a decapping pyrophosphatase activity exists in mammalian cells.

Using enzymatic assays, we demonstrated that the primary cleavage product is m^7GMP and that the lower spot is inorganic phosphate hydrolyzed from the m^7GMP. An aliquot of the products generated from a 30 min in vitro decay assay (Figure 3B, lane 2) was treated with nucleotide diphosphate kinase (NDPK) (lane 3). NDPK converts GDP to GTP but does not use GMP as a substrate. NDPK treatment had no effect on the accumulation of either spot (compare lane 2 to lane 3), indicating that the lower spot was not m^7GDP. As expected, the m^7GDP product produced by yeast Dcp1p (lane 4) was converted to m^7GTP by NDPK (lane 5). When the decay reactions were carried out in the presence of phosphatase inhibitors, the m^7GMP product was enriched (lane 6). Conversely, when the reaction products from lane 2 were treated with a phosphatase, the lower spot was enriched (lane 7). These data suggest that the slower migrating band is inorganic phosphate (^{32}Pi) released from the m^7GMP product by a phosphatase in the extract. Consistent with this conclusion, ^{32}Pi comigrates with the

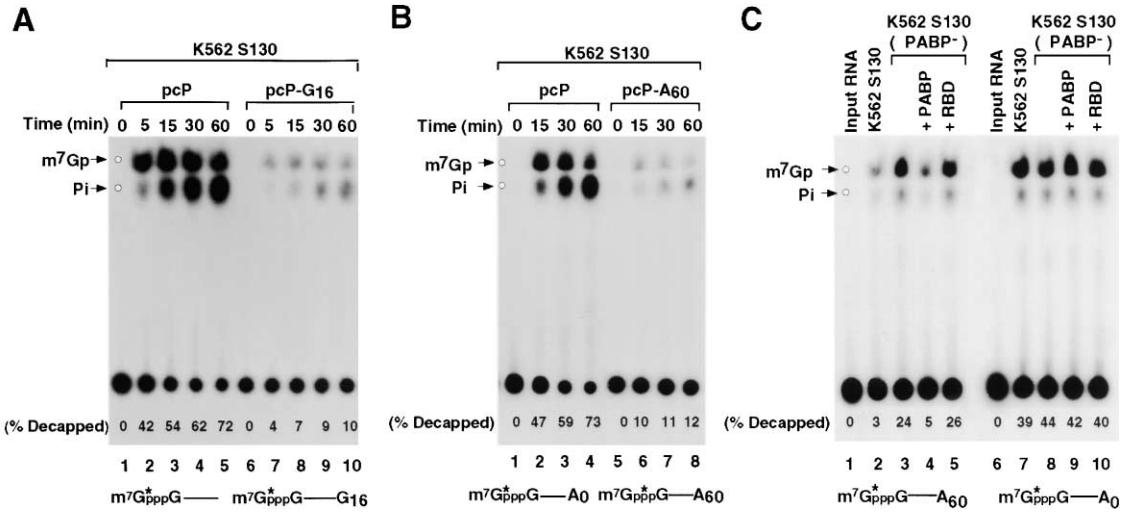

Figure 4. The DcpS Decapping Activity Is Dependent on 3′ to 5′ Degradation

(A) Cap-labeled RNAs lacking (lanes 1–5) or containing (lanes 6–10) a G_{16} track were used in an in vitro decay assay for the indicated times, and the products were resolved by TLC. Labeling is as described in the legend to Figure 3.

(B) Cap-labeled RNAs lacking (lanes 1–4) or containing (lanes 5–8) a poly(A) tail were used in an in vitro decay assay for the indicated times, and the products were resolved by TLC.

(C) Cap-labeled and polyadenylated (lanes 1–5) or unadenylated RNAs (lanes 6–10) were used in an in vitro decay assay for 10 min with K562 S130 extract or extract depleted of PABP ($PABP^-$), as marked. Recombinant PABP (15 pmol; lanes 4 and 9) or the RNA binding domain of hnRNP U (lanes 5 and 10) were added as indicated.

lower spot as well as the m^7GDP standard (lane 8). These data demonstrate the following: first, that m^7GMP is the primary cleavage product of the decapping activity, and second, that the product comigrating with the m^7GDP standard is not m^7GDP but instead is inorganic ^{32}Pi hydrolyzed from the original m^7GMP. We conclude that a pyrophosphatase activity is present in mammalian cells, which hydrolyzes the cap and releases m^7GMP.

The Decapping Activity Is Specific to the Methylated Cap Structure

The cap structure of all eukaryotic cellular mRNA contains a methyl group at the N-7 position of the terminal guanosine. The specificity of the pyrophosphatase activity for methylated cap was determined by a competition assay using methylated cap analog (m^7GpppG) or unmethylated cap analog (GpppG). As expected, addition of m^7GpppG competed for the decapping activity and reduced the accumulation of m^7GMP (Figure 3C, lanes 3 and 4). Competition with GpppG had no effect (lanes 5 and 6), demonstrating a requirement for the N-7 methyl group in the decapping specificity. Consistent with the methyl-specificity, capped RNA lacking the N-7 methyl group was not decapped by this activity (data not shown). Surprisingly, in addition to inhibiting the m^7GMP product formation, the m^7GpppG competitor stimulated a new product (lanes 3 and 4), which comigrates with cold m^7GpppG standard and the m^7GpppG cap structure released by Nuclease P1 treatment of the capped-labeled RNA (lane 7). We conclude the new spot is m^7GpppG. Accumulation of the m^7GpppG cap product in lanes 3 and 4 indicates that the exoribonuclease activity precedes decapping. Therefore, the RNA is initially degraded by a 3′ to 5′ exoribonuclease and subsequently decapped. Addition of the m^7GpppG cap competitor inhibits the subsequent decapping step, resulting in the accumulation of the exoribonuclease byproduct.

Dependence of the Decapping Activity on 3′ to 5′ Exoribonucleolytic Decay

We reasoned that if the decapping occurred following 3′ to 5′ degradation of the RNA, placement of the G track at the 3′ end to block exoribonuclease activity should inhibit decapping. Cap-labeled pcP and pcP-G_{16} RNAs were utilized in a time course in vitro decay reaction, and the products were resolved by TLC. As expected, the pcP RNA was efficiently decapped with 72% of the RNA decapped at the 1 hr time point (Figure 4A, lanes 1–5). However, the presence of the G_{16} track on the RNA efficiently inhibited decapping, with 10% decapping detected at the final time point (lanes 6–10). A direct correlation between the extent of RNA degradation and the accumulation of the decapping products was observed by using uniformly labeled RNA in an identical reaction (data not shown, similar to Figure 1B). Similarly, the presence of a poly(A) tail on the 3′ end also inhibited decapping (Figure 4B). Unadenylated RNA was consistently decapped at a rate at least 5-fold greater than that of polyadenylated RNA (compare lanes 2–4 with 6–8). As expected, reactions carried out with PABP-depleted extract, which facilitates deadenylation and subsequent degradation of the RNA (Wang et al., 1999; Wang and Kiledjian, 2000b), also resulted in a corresponding greater decapping activity (Figure 4C, lane 3); this was reversed upon the stabilization of the RNA with the addition of recombinant PABP (lane 4). We conclude that the decapping activity that releases m^7GMP functions on degraded RNA and is a scavenger activity that

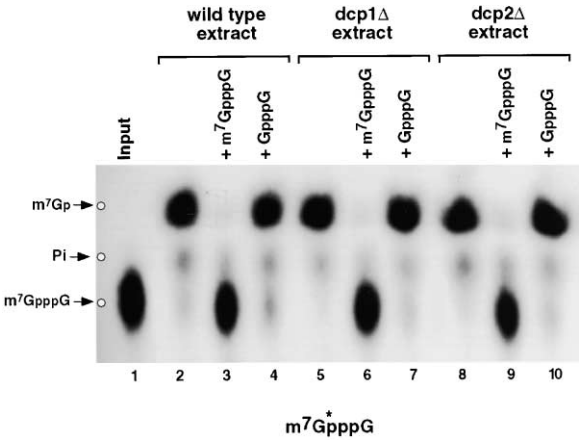

Figure 5. The Presence of DcpS in Yeast

Total yeast extract from wild-type (lanes 2–4), *dcp1*Δ (lanes 5–7), and *dcp2*Δ (lanes 8–10) strains were incubated with ^{32}P-labeled cap analog in standard in vitro decay conditions for 15 min, and the decapping products were detected by TLC. Added was 100 μM of methylated (m^7GpppG) or unmethylated (GpppG) cap competitor, as shown.

ultimately hydrolyzes the cap structure. We will refer to this activity as decapping scavenger (DcpS) activity.

The above data indicate that DcpS functions on mRNAs that have been degraded in the 3′ to 5′ direction. Since the alternative pathway for mRNA decay in yeast proceeds through 3′ to 5′ decay mediated by the exosome complex, we reasoned a DcpS activity should also be present in yeast. A ^{32}P-labeled cap analog (m^7G*pppG) generated by nuclease P1 digestion of cap-labeled RNA (as in Figure 3C, lane 7) was used as the substrate with yeast extract. The choice of this substrate was to distinguish between the DcpS activity that functions on cap analog and the well-characterized Dcp1p activity that does not hydrolyze this substrate. As shown in Figure 5, yeast extract contains a DcpS activity that releases m^7GMP (lane 2). As expected, the activity is sensitive to m^7GpppG competitor but not to GpppG competitor (lanes 3 and 4). The yeast DcpS activity is distinct from Dcp1p and Dcp2p, since strains containing a deletion of either gene encoding these proteins possess DcpS activity (lanes 5 and 8). The presence of DcpS in yeast suggests that this activity is conserved from yeast to mammals.

The Scavenger Decapping Activity Is Associated with a Subset of Exosome Proteins

Gel filtration was used to begin a biochemical analysis of the decapping activity. K562 S130 extract was resolved by a Superose 6 gel filtration column. To directly detect the DcpS activity, labeled cap analog was used as the substrate. As shown in the top panel of Figure 6A, DcpS activity elutes with a peak centered at fractions 63 and 64 in the 80–90 kDa size range. Unlabeled m^7GpppG competitor was included in these reactions to slow the decapping and enable detection of the most prominent peak. Otherwise, a broad peak extending to the 300 kDa range was detected (data not shown), suggesting that DcpS could also be in larger complexes. Interestingly, when the same fractions were tested with cap-labeled pcP RNA rather than the cap structure, the peak of DcpS activity was exclusively detected in the 300 kDa range. Since DcpS only functions on short capped oligonucleotides (Figure 3), these results suggest that exoribonuclease(s) and DcpS could both be associated within the same large complex.

An association between the DcpS and exosome proteins was next tested. The exosome complex was immunopurified with antibodies to two of the human exosome components, hRrp40p and hRrp41p (Ski6p) (Brouwer et al., 2001), as described in Experimental Procedures. ^{32}P-labeled cap analog was incubated with the immunopurified complex immobilized on the beads, and the reaction products were resolved by TLC. The cap analog was efficiently hydrolyzed to m^7GMP when using the complexes purified with antisera specific to hRrp40p and hRrp41p but not their respective preimmune sera (Figure 6B; compare lane 2 to lane 6 and lane 4 to lane 7). The interaction was also detected when using RNase-treated extract to preclude RNA tethering (lanes 3 and 5). Collectively, the association of DcpS with hRrp40p and hRrp41p in conjunction with the 300 kDa size of this complex implies that DcpS associates with a subset of exosome proteins that includes hRrp40p and hRrp41p.

Discussion

We present three findings pertaining to mammalian mRNA turnover in this report: first, the presence of a 5′ to 3′ exoribonuclease decay activity; second, the demonstration that 3′ to 5′ exoribonucleolytic decay is the major contributor to mRNA decay; and third, the presence of a degradation-dependent decapping pathway where a subset of exosome proteins are associated with DcpS.

Eukaryotes contain at least two distinct decapping activities. The first is Dcp1p, which hydrolyzes a capped RNA to release m^7GDP in yeast (Beelman et al., 1996; LaGrandeur and Parker, 1998). The second activity is the scavenger decapping activity reported in this study, which releases m^7GMP, is present in both mammals and yeast, and functions on the residual cap following degradation of the mRNA body. We believe the two decapping activities involve distinct proteins. First, Dcp1p and Dcp1p-like activities are resistant to cap analog competition (LaGrandeur and Parker, 1998), while the DcpS activity is efficiently inhibited by cap analog (Figure 3). Second, yeast strains lacking either Dcp1p or Dcp2p still contain DcpS activity (Figure 5). Third, in a parallel effort, we have cloned a gene encoding a human Dcp1-like decapping activity, which functions on capped RNA releasing m^7GDP but does not function on a cap analog (Z.W., X. Jiao, and M.K., unpublished data). Lastly, we more recently purified and cloned a human cDNA encoding a 40 kDa protein that possesses DcpS-like activity and hydrolyzes a cap analog to release m^7GMP (H. Liu, N. Rodgers, and M.K., unpublished data). The putative DcpS sequence was present in the database (GenBank accession number AF077201) and was originally obtained by sequencing novel cDNAs isolated from human $CD34^+$ hematopoietic stem/progenitor cells (HSPC015; Zhang et al., 2000). This putative DcpS protein does not contain any recognizable motifs or domains and is not homologous to any other human protein in the database. Collectively, these

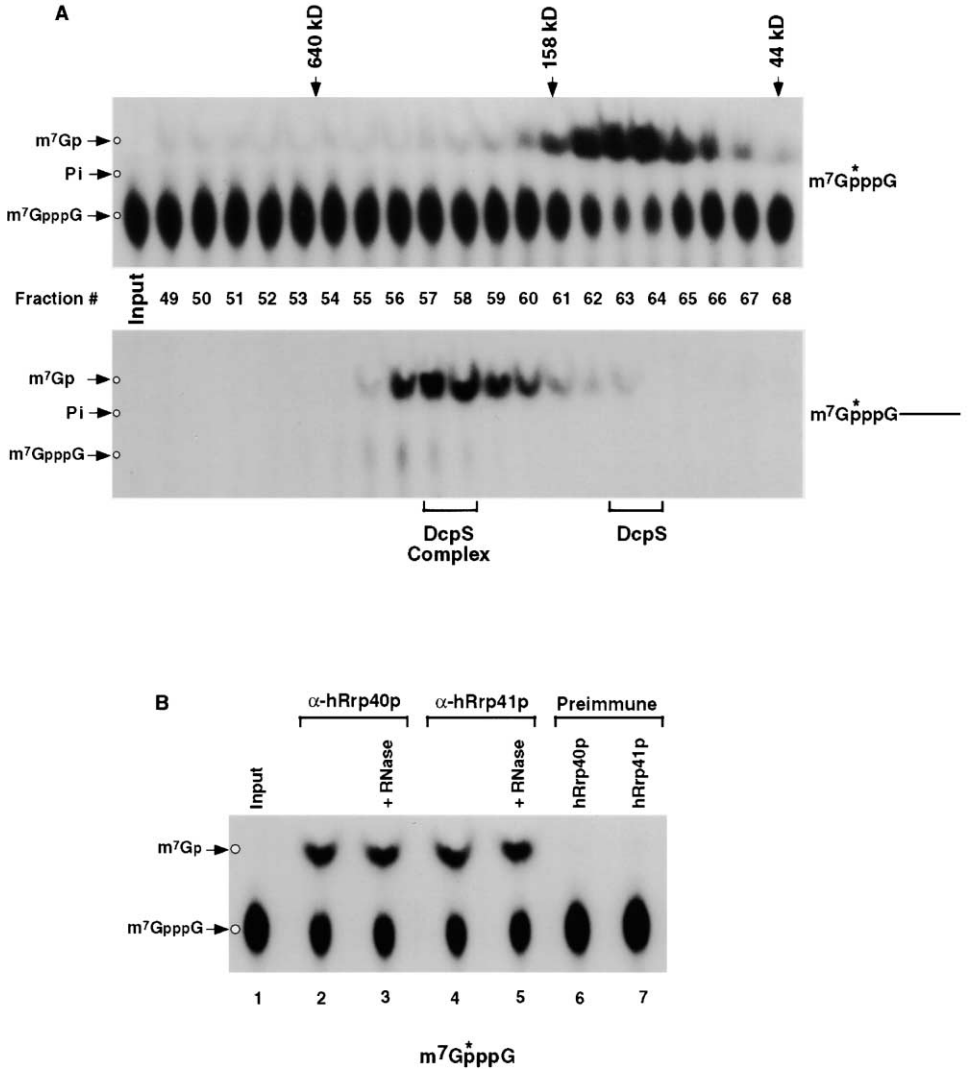

Figure 6. DcpS Can Exist in a 300 kDa Complex

(A) K562 S130 extract was fractionated on Superose 6, and aliquots from the indicated fractions were tested by an in vitro decay assay. The substrate used in the top image was ^{32}P-labeled cap analog (m^7G*pppG) to detect the DcpS activity directly, independent of prior exoribonucleolytic requirement. Cap-labeled pcP RNA was used as the substrate in the bottom image. The decapped products were resolved by TLC. The DcpS activity is detected at approximately 80 kDa when labeled cap analog is used and at approximately 300 kDa with cap-labeled RNA, suggesting that DcpS is associated with exoribonucleases in the larger complex. A schematic of the substrates is shown on the right, the position of the molecular weight standards is shown at the top, and the standards are represented on the left. The positions of the DcpS complex and free DcpS are indicated on the bottom.

(B) DcpS activity coimmunopurified with antisera to hRrp40p (αhRrp40p) and hRrp41p (αhRrp41p) from K562 S130 extract or extract pretreated with micrococcal nuclease (+RNase) using ^{32}P-labeled cap analog as substrate. The respective control preimmune sera coimmunopurifications are shown in lanes 6 and 7.

data support the presence of at least two distinct decapping proteins in eukaryotes.

Interestingly, a decapping activity similar to DcpS was initially identified over 25 years ago by Shatkin and colleagues (Nuss et al., 1975). The activity hydrolyzed capped oligonucleotides that were less than 10 nucleotides long but did not decap longer mRNAs (Nuss and Furuichi, 1977; Nuss et al., 1975). The 80 kDa size of DcpS activity by gel filtration (Figure 6A) is consistent with the size of the activity described by Nuss and Furuichi (1977), suggesting that both activities are the same. However, we anticipate that the 80 kDa size results from dimerization of the 40 kDa putative DcpS protein. The originally described activity was proposed to be a scavenger for capped oligonucleotide byproducts of 3′ to 5′ exoribonuclease degradation (Furuichi and Shatkin, 1989). Our data confirms the original hypothesis and demonstrates that DcpS can be associated within a 300 kDa complex that includes a subset of the 3′ to 5′ exonuclease proteins contained within the exosome.

A prominent role has been attributed to 5′ to 3′ exoribonuclease activity in yeast, where the major pathway involves deadenylation-dependent decapping followed by 5′ to 3′ exoribonuclease decay by the Xrn1 protein

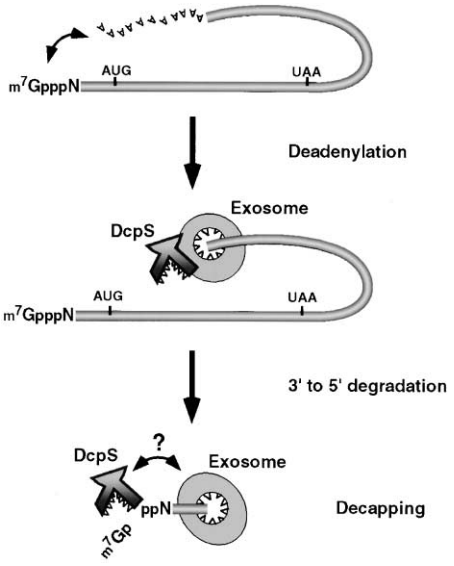

Figure 7. One Potential Pathway of mRNA Decay in Mammalian Cells

An mRNA with an interaction between the 5′ and 3′ termini is shown between the cap and poly(A) tail. Upon deadenylation, the major pathway involves 3′ to 5′ exoribonucleolytic degradation of the RNA by a complex consisting of DcpS and a subset of the exosome proteins. After degradation of the mRNA body, the resulting cap is hydrolyzed by DcpS.

(Beelman et al., 1996; Decker and Parker, 1994; LaGrandeur and Parker, 1998; Larimer et al., 1992; Muhlrad et al., 1995). An alternative pathway involving 3′ to 5′ exoribonuclease decay has also been demonstrated (Anderson and Parker, 1998). Despite the cloning of a mouse homolog of XRN1, (Bashkirov et al., 1997), a functional role for a 5′ to 3′ exoribonuclease activity has not previously been shown in mammalian mRNA decay. As shown in Figure 1, 5′ to 3′ exoribonuclease activity is functional in mammalian extract. However, the relative lower contribution of this activity in the decay of RNA both in cytosolic extract and in cells (Figures 1 and 2) suggests that degradation from the 5′ end is not a major contributor to overall mRNA decay.

The relative contributions of the two terminal exoribonucleases in mammalian mRNA decay appears to be opposite of that in yeast. We propose that a major pathway (perhaps the default pathway) is deadenylation followed by 3′ to 5′ degradation-dependent decapping, while an alternative pathway (possibly the regulatory pathway) involves deadenylation-dependent direct decapping. A model for the 3′ to 5′ mRNA degradation pathway is presented in Figure 7. Similar to yeast, the initial step in mammalian mRNA turnover involves deadenylation. This is supported by both in vivo data (Shyu et al., 1991; Wilson and Treisman, 1988) and in vitro data (Bernstein et al., 1989; Brewer, 1998; Ford et al., 1999; Wang et al., 1999). Following deadenylation, the prominent contribution of the 3′ to 5′ exoribonucleases (Figures 1 and 2) suggests that degradation of the mRNA from this direction is the more predominant pathway. The coimmunopurification of a subset of the exosome proteins with DcpS implies that DcpS is associated with exoribonucleases and is presented to the capped oligonucleotide following decay. DcpS contains a pyrophosphatase activity that decaps the 5′ end and releases m^7GMP. This model is particularly appealing because it provides one large complex that mediates degradation of the mRNA body and the hydrolysis of the 5′ cap to complete the demise of the mRNA. The presence of a DcpS activity in yeast (Figure 5) suggests that a functional link also exists between the yeast exosome proteins and DcpS. Curiously, yeast DcpS had not previously been reported. Perhaps this is because the substrate for DcpS results from the 3′ to 5′ decay process, which is a minor contributor to mRNA turnover in this organism.

Two additional pathways also exist in mammals, which have not been listed in Figure 7. The first involves deadenylation-dependent decapping of RNAs (Couttet et al., 1997). Our data suggests that this pathway is a minor contributor to mammalian mRNA decay. Consistent with this premise, Couttet et al. (1997) estimated that only 3% of deadenylated mRNAs were detected to be decapped by an mRNA circularization, RT-PCR assay. It is possible that this is a regulatory pathway that is more extensively utilized under specific cellular conditions. A second pathway (also not represented in the model) involves the initiation of degradation by endoribonucleases (Schoenberg and Chernokalskaya, 1997). Endoribonuclease cleavage can be independent of the poly(A) tail and cleave the mRNA while it is still polyadenylated (Binder et al., 1994; Brown et al., 1993; Stoeckle and Hanafusa, 1989) or are inhibited by the poly(A) tail and cleave after deadenylation (Wang and Kiledjian, 2000a).

The yeast 3′ to 5′ exoribonuclease exosome complex consists of 11 proteins within a 485 kDa complex as determined by the calculated molecular weights of the individual components (Allmang et al., 1999; Mitchell et al., 1997). Ten of these proteins are present in both the nucleus and cytoplasm while one, Rrp6p, is strictly nuclear. Similarly in humans, an exosome complex consisting of 11–16 proteins has been identified (Allmang et al., 1999; Gelpi et al., 1990; Reimer et al., 1986) where the Rrp6p homolog, PM/Scl 100, is restricted to the nucleus (Allmang et al., 1999). The association of DcpS with the hRrp40p and hRrp41p exosome proteins in a 300 kDa complex indicates that distinct subcomplexes of the exosome might exist. This is further supported by a broad distribution in the 250–700 kDa size range for the hRrp40p, hRrp41p, and hRrp46p (Brouwer et al., 2001) and the exclusion of PM/Scl-100 (Rrp6p) from the cytoplasmic exosome complex (Allmang et al., 1999; Brouwer et al., 2001). It is plausible that the functional mRNA-specific exosome subcomplex in the cytoplasm is 300 kDa and includes DcpS. However, it should be noted that the extract used in our experiments is a post-polysomal cytosolic extract. We cannot exclude the presence of another distinct complex(es) in the polysomal fraction.

Proteins that associate with and possibly regulate the specificity of the exosome have been reported. In yeast, the DEVH box protein Ski2p has been proposed to be a modulator of the exosome in mediating the specific decay of mRNA (Anderson and Parker, 1998). A second DEVH protein, Dob1p, was proposed to fulfill an analogous modulatory role on the exosome components in-

volved in 5.8S pre-rRNA processing (de la Cruz et al., 1998). The cap specificity of DcpS and the association of this protein with the exosome makes DcpS an attractive candidate as a regulator of the exosome complex responsible for mRNA decay. Further characterization of the putative DcpS protein will begin addressing this issue as well as how DcpS is regulated.

Experimental Procedures

RNA Production

The pcDNA3 polylinker (pcP) RNA was transcribed by T7 RNA polymerase from a PCR-generated template using the T7 and SP6 promoter primers. RNAs containing 60 adenosines or 16 guanosines at the 3′ end of the template were generated with a 3′ SP6 promoter primer containing 60 thymidines or 16 cytosines, respectively. RNAs containing an internal G_{16} track were similarly generated from PCR templates that used primers to insert 16 guanosines at nucleotide 96 of pcP. Uniformly labeled and capped RNAs were transcribed in vitro with T7 RNA polymerase in the presence of [α-^{32}P]UTP and m^7GpppG cap analog according to the manufacturer (Promega). Uniformly labeled and uncapped RNAs were similarly generated except that the m^7GpppG cap analog was omitted. In vitro transcribed, unlabeled, uncapped RNAs were cap labeled at the α-phosphate (relative to the terminal guanine; m^7G*pppG-) using the vaccinia virus capping enzyme (Shuman, 1990) with [α-^{32}P]GTP and S-adenosylmethionine (SAM), as described (Wang et al., 1999). All RNAs were gel purified prior to use as described (Wang et al., 1999).

Extract Preparation

Human erythroleukemia K562 cells and HeLa cells were obtained from Cellex Biosciences (Minneapolis, MN), and cytosolic S130 extract was prepared as described previously (Kiledjian et al., 1999). PABP-depleted extract was generated by repeated incubations with poly(A) Sepharose beads, as described (Wang et al., 1999). Yeast total extract was prepared according to Zhang et al. (1999b).

In Vitro RNA Decay Assays

In vitro mRNA decay assays were carried out at 37°C with 50 μg of S130 extract for the indicated times in IVDA buffer (10 mM Tris [pH 7.5], 100 mM potassium acetate, 2 mM magnesium acetate, 2 mM DTT, 10 mM creatine phosphate, 1 mM ATP, 0.4 mM GTP, and 0.1 mM Spermine), as previously described (Wang et al., 1999). Where indicated, a 1$\times$ phosphatase inhibitor cocktail (Phosphatase inhibitor cocktail 1 and 2; Sigma) was included in the decay reactions. Phosphatase treatment of the in vitro decay products was carried out with 10 units of calf intestinal alkaline phosphatase for 30 min as recommended by the manufacturer (NEB). For the NDPK reaction, the products of an in vitro decay reaction were phenol:chloroform (1:1) extracted once and chloroform extracted twice and subsequently treated with 1 unit NDPK (Sigma) for 30 min in the presence of 1 mM ATP. Decapping reactions using Dcp1p were carried out with 0.4 μg protein and 0.1 pmol cap-labeled RNA, as described in Zhang et al. (1999b),

Detection of Decapping Products

In vitro decay reactions were stopped and extracted once with an equal mixture of phenol:chloroform and twice with chloroform. An aliquot was spotted onto PEI-cellulose TLC plates (Sigma) that were prerun in H_20 and air dried prior to use and the products developed with 0.45 M $(NH_4)_2SO_4$ in a TLC chamber. The TLC plates were dried and exposed to Kodak BioMax film. Radiolabeled inorganic phosphate in Figure 3 was generated by treating a ^{32}P-end-labeled DNA oligonucleotide with calf intestinal phosphatase. All quantitations were conducted with a Molecular Dynamics Phosphoroimager (Storm860) using ImageQuant-5 software. Nuclease P1 (Roche) treatment of cap-labeled RNA was carried out with 1 unit enzyme in 10 mM Tris (pH 7.5) and 1 mM $ZnCl_2$ for 1 hr at 37°C.

Gel Filtration Chromatography

Gel filtration chromatography was carried out with 50 μl of K562 S130 extract (350 μg protein) on a Superose-6 gel filtration column (Amersham/Pharmacia). The column was equilibrated with 20 mM HEPES (pH 7.4) and 150 mM KCl. Collected were 250 μl fractions, and 20 μl from each fraction was assayed for decapping activity in IVDA buffer. One micromolar unlabeled cap analog was included in the reactions presented on the top panel of Figure 6A to slow the decapping reaction.

Immunoprecipitation

Immunoprecipitations were carried out with 10 μl of either specific antisera or preimmune sera bound to 20 μl protein A beads. K562 S130 extract (300 μg) was incubated with the antibody-coupled beads at 4°C for 2 hr in PBS containing 0.5% Triton X-100. Unbound proteins were removed with five washes of the same buffer and two washes with IVDA buffer. Where indicated, the extract was initially treated with micrococcal nuclease (400 units/ml) at 37°C for 20 min. The presence of DcpS activity was determined by using ^{32}P-labeled cap analog generated by Nuclease P1. The labeled cap analog was incubated with the immunopurified protein complex bound to the beads in IVDA buffer at 37°C for 20 min. The product was extracted once with phenol:chloroform (1:1) and twice with chloroform, and the supernatant was resolved by TLC.

Electroporation

Uniformly labeled RNA (2×10^7 cpm/0.5 μg) was electroporated into 10^7 K562 cells in a total volume of 400 μl PBS in a 4 mm gap cuvette using a BioRad Genepulser charged at 320V, 500μF. All reagents were kept on ice prior to electroporation. Following discharge, the cells were washed twice with PBS at room temperature, resuspended in prewarmed complete media, and placed at 37°C. Cells were harvested at the indicated times, washed twice in PBS, and lysed by vortexing in 300 μl lysis buffer (10 mM Tris [pH 7.4], 100 mM NaCl, 2.5 mM $MgCl_2$, and 0.5% Triton X-100), which was spiked with a ^{32}P-labeled oligonucleotide as an internal control for RNA precipitation and gel loading. The supernatant was extracted once with an equal mixture of phenol and chloroform and the RNA was ethanol precipitated and resolved on a 7 M urea/8% polyacrylamide denaturing gel.

RNase Protection Assays

RNase protection assays were carried out as previously described (Wang and Kiledjian, 2000a), using an antisense RNA to nucleotides 249–350 (5′ end) and to nucleotides 1829–2032 (3′ end) of the c-*myc* mRNA. The RNA were transcribed in the presence of [α-^{32}P]UTP from a PCR-generated template that inserted a T7 polymerase promoter on the 5′ end and 35 nucleotide uncomplementary sequence on the 3′ end.

Acknowledgments

We are indebted to H. Liu for providing unpublished results regarding the DcpS protein. We thank G.J.M. Pruijn and R. Raijmakers for the exosome antisera, C.J. Wilusz and S. Peltz for the Dcp1 protein, and R. Parker for the yeast strains. We also thank N.D. Rodgers, A. Shatkin, P. Trifillis, Y. Wen, G.J.M. Pruijn, R. Raijmakers, R. Parker, and C. Martin for helpful discussions and/or critical reading of the manuscript.

This work was supported by funds from the National Institutes of Health, grant DK51611 to M.K.

Received June 20, 2001; revised November 2, 2001.

References

Allmang, C., Petfalski, E., Podtelejnikov, A., Mann, M., Tollervey, D., and Mitchell, P. (1999). The yeast exosome and human PM-Scl are related complexes of 3′ → 5′ exonucleases. Genes Dev. *13*, 2148–2158.

Anderson, J.S.J., and Parker, R.P. (1998). The 3′ to 5′ degradation of yeast mRNAs is a general mechanism for mRNA turnover that requires the SKI2 DEVH box protein and 3′ to 5′ exonucleases of the exosome complex. EMBO J. *17*, 1497–1506.

Bashkirov, V.I., Scherthan, H., Solinger, J.A., Buerstedde, J.M., and Heyer, W.D. (1997). A mouse cytoplasmic exoribonuclease

(mXRN1p) with preference for G4 tetraplex substrates. J. Cell Biol. *136*, 761–773.

Beelman, C.A., Stevens, A., Caponigro, G., LaGrandeur, T.E., Hatfield, L., Fortner, D.M., and Parker, R. (1996). An essential component of the decapping enzyme required for normal rates of mRNA turnover. Nature *382*, 642–646.

Bernstein, P., Peltz, S.W., and Ross, J. (1989). The poly(A)-poly(A)-binding protein complex is a major determinant of mRNA stability in vitro. Mol. Cell. Biol. *9*, 659–670.

Binder, R., Horowitz, J.A., Basilion, J.P., Koeller, D.M., Klausner, R.D., and Harford, J.B. (1994). Evidence that the pathway of transferrin receptor mRNA degradation involves an endonucleolytic cleavage within the 3′ UTR and does not involve poly(A) tail shortening. EMBO J. *13*, 1969–1980.

Bonnerot, C., Boeck, R., and Lapeyre, B. (2000). The two proteins Pat1p (Mrt1p) and Spb8p interact in vivo, are required for mRNA decay, and are functionally linked to Pab1p. Mol. Cell. Biol. *20*, 5939–5946.

Bousquet-Antonelli, C., Presutti, C., and Tollervey, D. (2000). Identification of a regulated pathway for nuclear pre-mRNA turnover. Cell *102*, 765–775.

Bouveret, E., Rigaut, G., Shevchenko, A., Wilm, M., and Seraphin, B. (2000). A Sm-like protein complex that participates in mRNA degradation. EMBO J *19*, 1661–1671.

Brewer, G. (1998). Characterization of c-myc 3′ to 5′ mRNA decay activities in an in vitro system. J. Biol. Chem. *273*, 34770–34774.

Brouwer, R., Allmang, C., Raijmakers, R., van Aarssen, Y., Egberts, W.V., Petfalski, E., van Venrooij, W.J., Tollervey, D., and Pruijn, G.J. (2001). Three novel components of the human exosome. J. Biol. Chem. *276*, 6177–6184.

Brown, B.D., Zipkin, I.D., and Harland, R.M. (1993). Sequence-specific endonucleolytic cleavage and protection of mRNA in Xenopus and Drosophila. Genes Dev. *7*, 1620–1631.

Couttet, P., Fromont-Racine, M., Steel, D., Pictet, R., and Grange, T. (1997). Messenger RNA deadenylylation precedes decapping in mammalian cells. Proc. Natl. Acad. Sci. USA *94*, 5628–5633.

de la Cruz, J., Kressler, D., Tollervey, D., and Linder, P. (1998). Dob1p (Mtr4p) is a putative ATP-dependent RNA helicase required for the 3′ end formation of 5.8S rRNA in Saccharomyces cerevisiae. EMBO J. *17*, 1128–1140.

Decker, C.J., and Parker, R. (1993). A turnover pathway for both stable and unstable mRNAs in yeast: evidence for a requirement for deadenylation. Genes Dev. *7*, 1632–1643.

Decker, C.J., and Parker, R. (1994). Mechanisms of mRNA degradation in eukaryotes. Trends Biochem. Sci. *19*, 336–340.

Drummond, D.R., Armstrong, J., and Colman, A. (1985). The effect of capping and polyadenylation on the stability, movement and translation of synthetic messenger RNAs in Xenopus oocytes. Nucleic Acids Res. *13*, 7375–7394.

Dunckley, T., and Parker, R. (1999). The DCP2 protein is required for mRNA decapping in Saccharomyces cerevisiae and contains a functional MutT motif. EMBO J. *18*, 5411–5422.

Ford, L.P., Watson, J., Keene, J.D., and Wilusz, J. (1999). ELAV proteins stabilize deadenylated intermediates in a novel in vitro mRNA deadenylation/degradation system. Genes Dev. *13*, 188–201.

Furuichi, Y., and Shatkin, A.J. (1989). Characterization of cap structures. Methods Enzymol. *180*, 164–176.

Furuichi, Y., and Shatkin, A.J. (2000). Viral and cellular mRNA capping: past and prospects. Adv. Virus Res. *55*, 135–184.

Furuichi, Y., LaFiandra, A., and Shatkin, A.J. (1977). 5′-terminal structure and mRNA stability. Nature *266*, 235–239.

Gao, M., Wilusz, C.J., Peltz, S.W., and Wilusz, J. (2001). A novel mRNA-decapping activity in HeLa cytoplasmic extracts is regulated by AU-rich elements. EMBO J. *20*, 1134–1143.

Gelpi, C., Alguero, A., Angeles Martinez, M., Vidal, S., Juarez, C., and Rodriguez-Sanchez, J.L. (1990). Identification of protein components reactive with anti-PM/Scl autoantibodies. Clin. Exp. Immunol. *81*, 59–64.

Gingras, A.C., Raught, B., and Sonenberg, N. (1999). eIF4 initiation factors: effectors of mRNA recruitment to ribosomes and regulators of translation. Annu. Rev. Biochem. *68*, 913–963.

Green, M.R., Maniatis, T., and Melton, D.A. (1983). Human beta-globin pre-mRNA synthesized in vitro is accurately spliced in Xenopus oocyte nuclei. Cell *32*, 681–694.

Hentze, M.W. (1997). eIF4G: a multipurpose ribosome adapter? Science *275*, 500–501.

Hsu, C.L., and Stevens, A. (1993). Yeast cells lacking 5′→3′ exoribonuclease 1 contain mRNA species that are poly(A) deficient and partially lack the 5′ cap structure. Mol. Cell. Biol. *13*, 4826–4835.

Izaurralde, E., Lewis, J., McGuigan, C., Jankowska, M., Darzynkiewicz, E., and Mattaj, I.W. (1994). A nuclear cap binding protein complex involved in pre-mRNA splicing. Cell *78*, 657–668.

Izaurralde, E., Lewis, J., Gamberi, C., Jarmolowski, A., McGuigan, C., and Mattaj, I.W. (1995). A cap-binding protein complex mediating U snRNA export. Nature *376*, 709–712.

Jarmolowski, A., Boelens, W.C., Izaurralde, E., and Mattaj, I.W. (1994). Nuclear export of different classes of RNA is mediated by specific factors. J. Cell Biol. *124*, 627–635.

Kiledjian, M., Day, N., and Trifillis, P. (1999). Purification and RNA binding properties of the polycytidylate-binding proteins alphaCP1 and alphaCP2. Methods *17*, 84–91.

Konarska, M.M., Padgett, R.A., and Sharp, P.A. (1984). Recognition of cap structure in splicing in vitro of mRNA precursors. Cell *38*, 731–736.

Krieg, P.A., and Melton, D.A. (1984). Functional messenger RNAs are produced by SP6 in vitro transcription of cloned cDNAs. Nucleic Acids Res. *12*, 7057–7070.

LaGrandeur, T.E., and Parker, R. (1998). Isolation and characterization of Dcp1p, the yeast mRNA decapping enzyme. EMBO J. *17*, 1487–1496.

Larimer, F.W., Hsu, C.L., Maupin, M.K., and Stevens, A. (1992). Characterization of the XRN1 gene encoding a 5′→3′ exoribonuclease: sequence data and analysis of disparate protein and mRNA levels of gene-disrupted yeast cells. Gene *120*, 51–57.

Mitchell, P., Petfalski, E., Shevchenko, A., Mann, M., and Tollervey, D. (1997). The exosome: a conserved eukaryotic RNA processing complex containing multiple 3′→5′ exoribonucleases. Cell *91*, 457–466.

Muhlrad, D., Decker, C.J., and Parker, R. (1994). Deadenylation of the unstable mRNA encoded by the yeast MFA2 gene leads to decapping followed by 5′→3′ digestion of the transcript. Genes Dev. *8*, 855–866.

Muhlrad, D., Decker, C.J., and Parker, R. (1995). Turnover mechanisms of the stable yeast PGK1 mRNA. Mol. Cell. Biol. *15*, 2145–2156.

Nuss, D.L., and Furuichi, Y. (1977). Characterization of the m7G(5′)pppN-pyrophosphatase activity from HeLa cells. J. Biol. Chem. *252*, 2815–2821.

Nuss, D.L., Furuichi, Y., Koch, G., and Shatkin, A.J. (1975). Detection in HeLa cell extracts of a 7-methyl guanosine specific enzyme activity that cleaves m7GpppNm. Cell *6*, 21–27.

Reimer, G., Scheer, U., Peters, J.M., and Tan, E.M. (1986). Immunolocalization and partial characterization of a nucleolar autoantigen (PM-Scl) associated with polymyositis/scleroderma overlap syndromes. J. Immunol. *137*, 3802–3808.

Ross, J. (1995). mRNA stability in mammalian cells. Microbiol. Rev. *59*, 423–450.

Sachs, A.B. (1993). Messenger RNA degradation in eukaryotes. Cell *74*, 413–421.

Sachs, A.B., Sarnow, P., and Hentze, M.W. (1997). Starting at the beginning, middle, and end: translation initiation in eukaryotes. Cell *89*, 831–838.

Schoenberg, D.R., and Chernokalskaya, E. (1997). Ribonucleases involved in eukaryotic mRNA turnover. In mRNA Metabolism and Post-Transcriptional Gene Regulation, J.B. Harford and D.R. Morris, eds. (New York: Wiley-Liss, Inc.), pp. 217–240.

Shatkin, A.J. (1976). Capping of eucaryotic mRNAs. Cell *9*, 645–653.

Shuman, S. (1990). Catalytic activity of vaccinia mRNA capping enzyme subunits coexpressed in Escherichia coli. J. Biol. Chem. *265*, 11960–11966.

Shyu, A.B., Belasco, J.G., and Greenberg, M.E. (1991). Two distinct destabilizing elements in the c-fos message trigger deadenylation as a first step in rapid mRNA decay. Genes Dev. *5*, 221–231.

Stoeckle, M.Y., and Hanafusa, H. (1989). Processing of 9E3 mRNA and regulation of its stability in normal and Rous sarcoma virus-transformed cells. Mol. Cell. Biol. *9*, 4738–4745.

Wang, Z., and Kiledjian, M. (2000a). Identification of an erythroid-enriched endoribonuclease activity involved in specific mRNA cleavage. EMBO J. *19*, 295–305.

Wang, Z., and Kiledjian, M. (2000b). The poly(A)-binding protein and an mRNA stability protein jointly regulate an endoribonuclease activity. Mol. Cell. Biol. *20*, 6334–6341.

Wang, Z., Day, N., Trifillis, P., and Kiledjian, M. (1999). An mRNA stability complex functions with poly(A)-binding protein to stabilize mRNA in vitro. Mol. Cell. Biol. *19*, 4552–4560.

Wickens, M.P., and Gurdon, J.B. (1983). Post-transcriptional processing of simian virus 40 late transcripts in injected frog oocytes. J. Mol. Biol. *163*, 1–26.

Wilson, T., and Treisman, R. (1988). Removal of poly(A) and consequent degradation of c-fos mRNA facilitated by 3′ AU-rich sequences. Nature *336*, 396–399.

Zhang, S., Williams, C.J., Hagan, K., and Peltz, S.W. (1999a). Mutations in VPS16 and MRT1 stabilize mRNAs by activating an inhibitor of the decapping enzyme. Mol. Cell. Biol. *19*, 7568–7576.

Zhang, S., Williams, C.J., Wormington, M., Stevens, A., and Peltz, S.W. (1999b). Monitoring mRNA decapping activity. Methods *17*, 46–51.

Zhang, Q.H., Ye, M., Wu, X.Y., Ren, S.X., Zhao, M., Zhao, C.J., Fu, G., Shen, Y., Fan, H.Y., Lu, G., et al. (2000). Cloning and functional analysis of cDNAs with open reading frames for 300 previously undefined genes expressed in CD34+ hematopoietic stem/progenitor cells. Genome Res. *10*, 1546–1560.